Chaos, Solitons and Fractals 42 (2009) 784–791

Contents lists available at ScienceDirect

Chaos, Solitons and Fractals

journal homepage: www.elsevier.com/locate/chaos

Chaos control using an adaptive fuzzy sliding mode controller with application to a nonlinear pendulum

Wallace M. Bessa [a], Aline S. de Paula [b], Marcelo A. Savi [b,*]

[a] Universidade Federal do Rio Grande do Norte, Department of Mechanical Engineering, Campus Universitário Lagoa Nova, 59072-970 Natal, RN, Brazil
[b] Universidade Federal do Rio de Janeiro, COPPE – Department of Mechanical Engineering, P.O. Box 68.503, 21941-972 Rio de Janeiro, RJ, Brazil

ARTICLE INFO

Article history:
Accepted 9 February 2009

ABSTRACT

Chaos control may be understood as the use of tiny perturbations for the stabilization of unstable periodic orbits embedded in a chaotic attractor. The idea that chaotic behavior may be controlled by small perturbations of physical parameters allows this kind of behavior to be desirable in different applications. In this work, chaos control is performed employing a variable structure controller. The approach is based on the sliding mode control strategy and enhanced by an adaptive fuzzy algorithm to cope with modeling inaccuracies. The convergence properties of the closed-loop system are analytically proven using Lyapunov's direct method and Barbalat's lemma. As an application of the control procedure, a nonlinear pendulum dynamics is investigated. Numerical results are presented in order to demonstrate the control system performance. A comparison between the stabilization of general orbits and unstable periodic orbits embedded in chaotic attractor is carried out showing that the chaos control can confer flexibility to the system by changing the response with low power consumption.

1. Introduction

Chaotic response is related to a dense set of unstable periodic orbits (UPOs) and the system often visits the neighborhood of each one of them. Moreover, chaos has sensitive dependence to initial conditions, which implies that the system evolution may be altered by small perturbations. Chaos control is based on the richness of chaotic behavior and may be understood as the use of tiny perturbations for the stabilization of an UPO embedded in a chaotic attractor. It makes this kind of behavior to be desirable in a variety of applications, since one of these UPO can provide better performance than others in a particular situation.

The first chaos control method has been proposed by Ott et al. [1], nowadays known as the OGY (Ott–Grebogi–Yorke) method. This is a discrete technique that considers small perturbations applied in one system parameter when the trajectory visits the neighborhood of the desired orbit when crossing a specific surface, such as some Poincaré section. The delayed feedback control [2], on the other hand, was the first continuous method proposed for controlling chaos, which states that chaotic systems can be stabilized by a feedback perturbation proportional to the difference between the present and the delayed state of the system.

Since the beginning of chaos control studies in the 1990's, many alternative methods were proposed in order to overcome some limitations of the original techniques. Pyragas [3] presents a review about improvements and applications of time-delayed feedback control. Based on OGY method, Dressler and Nitsche [4], Hübinger et al. [5], Korte et al. [6], Otani and Jones [7], So and Ott [8] and De Paula and Savi [9] suggest some improvements. Savi et al. [10] discusses some of these alternatives.

* Corresponding author.
E-mail addresses: wmbessa@ufrnet.br (W.M. Bessa), alinesp27@gmail.com (A.S. de Paula), savi@mecanica.ufrj.br (M.A. Savi).

0960-0779/$ - see front matter © 2009 Elsevier Ltd. All rights reserved.
doi:10.1016/j.chaos.2009.02.009

Literature presents some contributions related to the analysis of chaos control in mechanical systems. Andrievskii and Fradkov [11] present an overview of applications of chaos control in various scientific fields. Mechanical systems are included in this discussion presenting control of pendulums, beams, plates, friction, vibroformers, microcantilevers, cranes, and vessels. Savi et al. [10] also present an overview of some mechanical system chaos control that includes system with dry friction [12], impact [13] and system with non-smooth restoring forces [14]. Spano et al. [15] explores the idea of chaos control applied to intelligent systems while Macau [16] shows that chaos control techniques can be used in spacecraft orbits. Pendulum systems are analyzed in [17–20] using different approaches. De Paula and Savi [9] propose a multiparameter semi-continuous method based on OGY approach to perform the chaos control of a nonlinear pendulum. Afterwards, De Paula and Savi [21] use a continuous time delayed-feedback controller to control chaos in the same nonlinear pendulum.

This article proposes a robust controller to stabilize dynamical system UPOs based on the sliding mode control strategy and enhanced by a stable adaptive fuzzy inference system to cope with modeling imprecisions. The convergence properties of the tracking error are analytically proven using Lyapunov's direct method and Barbalat's lemma. As an application of the general procedure, the chaos control of a nonlinear pendulum that has a rich response, presenting chaos and transient chaos [22], is treated. Numerical simulations are carried out illustrating the stabilization of some UPOs of the chaotic attractor showing an effective response. Unstructured uncertainties related to unmodeled dynamics and structured uncertainties associated with parametric variations are both considered in the robustness analysis. Moreover, a comparison between the stabilization of general orbits and unstable periodic orbits embedded in chaotic attractor are performed showing the less energy consumption related to UPOs.

2. Adaptive fuzzy sliding mode control

As demonstrated by Bessa and Barrêto [23], adaptive fuzzy algorithms can be properly embedded in smooth sliding mode controllers to compensate for modeling inaccuracies, in order to improve the trajectory tracking of uncertain nonlinear systems. It has also been shown that adaptive fuzzy sliding mode controllers are suitable for a variety of applications ranging from remotely operated underwater vehicles [24] to space satellites [25].

On this basis, let us consider a second order dynamical system represented by the following equation of motion:

$$\ddot{\phi} = f(\phi, \dot{\phi}, t) + hu + p(\phi, \dot{\phi}) \tag{1}$$

where ϕ and $\dot{\phi}$ represent the state variables, u is the control input, h is the control gain, $f : \mathbb{R}^3 \to \mathbb{R}$ is a nonlinear function that represents system dynamics and p represents modeling inaccuracies.

Now, let $S(t)$ be a sliding surface defined in the state space by the equation $s(e, \dot{e}) = 0$, with the function $s : \mathbb{R}^2 \to \mathbb{R}$ satisfying

$$s(e, \dot{e}) = \dot{e} + \lambda e \tag{2}$$

where $e = \phi - \phi_d$ is the tracking error, $\dot{e}$ is the first time derivative of e, ϕ_d is the desired trajectory and λ is a strictly positive constant.

The control of the system dynamics (1) is done by assuming a sliding mode based approach, defining a control law composed by an equivalent control $\hat{u} = \hat{h}^{-1}(-\hat{f} - \hat{p} + \ddot{\phi}_d - \lambda\dot{e})$ and a discontinuous term $-K\,\mathrm{sgn}(s)$:

$$u = \hat{h}^{-1}(-\hat{f} - \hat{p} + \ddot{\phi}_d - \lambda\dot{e}) - K\,\mathrm{sgn}(s) \tag{3}$$

where $\hat{h}$, $\hat{f}$, and $\hat{p}$ are estimates of h, f and p, respectively, K is a positive control gain and $\mathrm{sgn}(\cdot)$ is defined as

$$\mathrm{sgn}(s) = \begin{cases} -1 & \text{if} \quad s < 0 \\ 0 & \text{if} \quad s = 0 \\ +1 & \text{if} \quad s > 0 \end{cases} \tag{4}$$

Regarding the development of the control law, the following assumptions should be made:

Assumption 1. The states ϕ and $\dot{\phi}$ are available.

Assumption 2. The desired trajectories ϕ_d and $\dot{\phi}_d$ are once differentiable in time. Furthermore ϕ_d, $\dot{\phi}_d$ and $\ddot{\phi}_d$ are available and with known bounds.

Assumption 3. The function f is unknown but bounded, i.e., $|\hat{f} - f| \leqslant \mathscr{F}$.

Assumption 4. The input gain h is unknown but positive and bounded, i.e., $0 < h_{\min} \leqslant h \leqslant h_{\max}$.

Assumption 5. The term p is unknown but bounded, i.e., $|p| \leqslant \mathscr{P}$.

Based on Assumption 4 and considering that the estimate $\hat{h}$ could be chosen according to the geometric mean $\hat{h} = \sqrt{h_{\max} h_{\min}}$, the bounds of h may be expressed as $\mathscr{H}^{-1} \leqslant \hat{h}/h \leqslant \mathscr{H}$, where $\mathscr{H} = \sqrt{h_{\max}/h_{\min}}$.

Under this condition, the gain K should be chosen according to

$$K \geqslant \mathscr{H}\hat{h}^{-1}(\eta + |\hat{p}| + \mathscr{P} + \mathscr{F}) + (\mathscr{H} - 1)|\hat{u}| \tag{5}$$

here η is a strictly positive constant related to the reaching time.

At this point, it should be highlighted that the control law (3), together with (5), is sufficient to impose the sliding condition

$$\frac{1}{2}\frac{d}{dt}s^2 \leqslant -\eta|s| \tag{6}$$

and, consequently, the finite time convergence to the sliding surface S.

In order to obtain a good approximation to p, the estimate $\hat{p}$ is computed directly by an adaptive fuzzy algorithm. The adopted fuzzy inference system is the zero order TSK (Takagi–Sugeno–Kang), whose rules can be stated in a linguistic manner as follows:

If ϕ is Φ_r and $\dot{\phi}$ is $\dot{\Phi}_r$ then $\hat{p} = \widehat{P}_r, \quad r = 1, 2, \ldots, N$

where Φ_r and $\dot{\Phi}_r$ are fuzzy sets, whose membership functions could be properly chosen, and $\widehat{P}_r$ is the output value of each one of the N fuzzy rules.

Considering that each rule defines a numerical value as output $\widehat{P}_r$, the final output $\hat{p}$ can be computed by a weighted average:

$$\hat{p}(\phi, \dot{\phi}) = \widehat{\mathbf{P}}^{\mathrm{T}}\boldsymbol{\Psi}(\phi, \dot{\phi}) \tag{7}$$

where $\widehat{\mathbf{P}} = [\widehat{P}_1, \widehat{P}_2, \ldots, \widehat{P}_N]$ is the vector containing the attributed values $\widehat{P}_r$ to each rule r, $\boldsymbol{\Psi}(\phi, \dot{\phi}) = [\psi_1, \psi_2, \ldots, \psi_N]$ is a vector with components $\psi_r(\phi, \dot{\phi}) = w_r / \sum_{r=1}^{N} w_r$ and w_r is the firing strength of each rule, which can be computed from the membership values with any fuzzy intersection operator (t-norm).

The estimation of $\hat{p}$ is done by considering that the vector of adjustable parameters can be automatically updated by the following adaptation law:

$$\dot{\widehat{\mathbf{P}}} = \varphi s\boldsymbol{\Psi}(\phi, \dot{\phi}) \tag{8}$$

where φ is a strictly positive constant related to the adaptation rate.

It is important to emphasize that the chosen adaptation law, Eq. (8), must not only provide a good approximation to p but also assure the convergence of the state variables to the sliding surface $S(t)$, for the purpose of trajectory tracking. In this way, in order to evaluate the stability of the closed-loop system, let a positive-definite function V be defined as

$$V(t) = \frac{1}{2}s^2 + \frac{1}{2\varphi}\boldsymbol{\delta}^{\mathrm{T}}\boldsymbol{\delta} \tag{9}$$

where $\boldsymbol{\delta} = \widehat{\mathbf{P}} - \widehat{\mathbf{P}}^*$ and $\widehat{\mathbf{P}}^*$ is the optimal parameter vector, associated with the optimal estimate $\hat{p}^*$. Hence, the time derivative of V is

$$\begin{aligned}\dot{V}(t) &= s\dot{s} + \varphi^{-1}\boldsymbol{\delta}^{\mathrm{T}}\dot{\boldsymbol{\delta}} = (\ddot{\phi} - \ddot{\phi}_d + \lambda\dot{e})s + \varphi^{-1}\boldsymbol{\delta}^{\mathrm{T}}\dot{\boldsymbol{\delta}} = (f + hu + p - \ddot{\phi}_d + \lambda\dot{e})s + \varphi^{-1}\boldsymbol{\delta}^{\mathrm{T}}\dot{\boldsymbol{\delta}} \\ &= \left[f + h\hat{h}^{-1}(-\hat{f} - \hat{p} + \ddot{\phi}_d - \lambda\dot{e}) - hK\mathrm{sgn}(s) + p - \ddot{\phi}_d + \lambda\dot{e}\right]s + \varphi^{-1}\boldsymbol{\delta}^{\mathrm{T}}\dot{\boldsymbol{\delta}}\end{aligned}$$

Defining a minimum approximation error as $\varepsilon = \hat{p}^* - p$, recalling that $\hat{u} = \hat{h}^{-1}(-\hat{f} - \hat{p} + \ddot{\phi}_d - \lambda\dot{e})$ and noting that $\dot{\boldsymbol{\delta}} = \dot{\widehat{\mathbf{P}}}$, $f = \hat{f} - (\hat{f} - f)$ and $p = \hat{p} - (\hat{p} - p)$, $\dot{V}$ becomes:

$$\begin{aligned}\dot{V}(t) &= -\left[(\hat{f} - f) + \varepsilon + (\hat{p} - \hat{p}^*) + \hat{h}\hat{u} - h\hat{u} + hK\mathrm{sgn}(s)\right]s + \varphi^{-1}\boldsymbol{\delta}^{\mathrm{T}}\dot{\widehat{\mathbf{P}}} \\ &= -\left[(\hat{f} - f) + \varepsilon + \boldsymbol{\delta}^{\mathrm{T}}\boldsymbol{\Psi}(\phi, \dot{\phi}) + \hat{h}\hat{u} - h\hat{u} + hK\mathrm{sgn}(s)\right]s + \varphi^{-1}\boldsymbol{\delta}^{\mathrm{T}}\dot{\widehat{\mathbf{P}}} \\ &= -\left[(\hat{f} - f) + \varepsilon + \hat{h}\hat{u} - h\hat{u} + hK\mathrm{sgn}(s)\right]s + \varphi^{-1}\boldsymbol{\delta}^{\mathrm{T}}\left[\dot{\widehat{\mathbf{P}}} - \varphi s\boldsymbol{\Psi}(\phi, \dot{\phi})\right]\end{aligned}$$

By applying the adaptation law, Eq. (8), to $\dot{\widehat{\mathbf{P}}}$, one has

$$\dot{V}(t) = -\left[(\hat{f} - f) + \varepsilon + \hat{h}\hat{u} - h\hat{u} + hK\mathrm{sgn}(s)\right]s \tag{10}$$

Furthermore, considering Assumptions 1–5, defining K according to (5) and verifying that $|\varepsilon| = |\hat{p}^* - p| \leqslant |\hat{p} - p| \leqslant |\hat{p}| + \mathscr{P}$, it follows that

$$\dot{V}(t) \leqslant -\eta|s| \tag{11}$$

which implies $V(t) \leqslant V(0)$ and that s and $\boldsymbol{\delta}$ are bounded.

Integrating both sides of (11) shows that

$$\lim_{t\to\infty}\int_0^t \eta|s|d\tau \leqslant \lim_{t\to\infty}[V(0) - V(t)] \leqslant V(0) < \infty$$

Now, since the absolute value function is uniformly continuous, Barbalat's lemma is evoked establishing that $s \to 0$ as $t \to \infty$, which ensures the convergence of the states to the sliding surface $S(t)$ and to the desired trajectory.

In spite of the demonstrated properties of the controller, the presence of a discontinuous term in the control law leads to the well-known chattering phenomenon. In order to overcome the undesirable chattering effects, a thin boundary layer, S_ϵ, in the neighborhood of the switching surface can be adopted [26]:

$$S_\epsilon = \{(e, \dot{e}) \in \mathbb{R}^2 || s(e, \dot{e})| \leqslant \epsilon\}$$

where ϵ is a strictly positive constant that represents the boundary layer thickness.

The boundary layer is achieved by replacing the sign function by a continuous interpolation inside S_ϵ. There are several options to smooth out the ideal relay but the most common choice is the saturation function:

$$\text{sat}(s/\epsilon) = \begin{cases} \text{sgn}(s) & \text{if} \quad |s/\epsilon| \geqslant 1 \\ s/\epsilon & \text{if} \quad |s/\epsilon| < 1 \end{cases}$$

In this way, to avoid chattering, a smooth version of Eq. (3) is defined:

$$u = \hat{h}^{-1}(-\hat{f} - \hat{p} + \ddot{\phi}_d - \lambda \dot{e}) - K \,\text{sat}(s/\epsilon) \tag{12}$$

Nevertheless, it should be emphasized that the substitution of the discontinuous term by a smooth approximation inside the boundary layer turns the perfect tracking into a tracking with guaranteed precision problem, which actually means that a steady-state error will always remain. According to Bessa [27] and considering a second order system with a smooth sliding mode controller, the tracking error vector will exponentially converge to a closed region $\Lambda = \{(e, \dot{e}) \in \mathbb{R}^2 || s(e, \dot{e})| \leqslant \epsilon$ and $|e| \leqslant \lambda^{-1}\epsilon$ and $|\dot{e}| \leqslant 2\epsilon\}$.

3. Nonlinear pendulum

As an application of the control procedure, a nonlinear pendulum is investigated. This pendulum is based on an experimental set up, previously analyzed by Franca and Savi [28] and Pereira–Pinto et al. [17]. De Paula et al. [22] presented a mathematical model to describe the dynamical behavior of the pendulum and the corresponding experimentally obtained parameters.

The schematic picture of the considered nonlinear pendulum is shown in Fig. 1. Basically, the pendulum consists of an aluminum disc (1) with a lumped mass (2) that is connected to a rotary motion sensor (4). This assembly is driven by a string-spring device (6) that is attached to an electric motor (7) and also provides torsional stiffness to the system. A magnetic device (3) provides an adjustable dissipation of energy. An actuator (5) provides the necessary perturbations to stabilize this system by properly changing the string length.

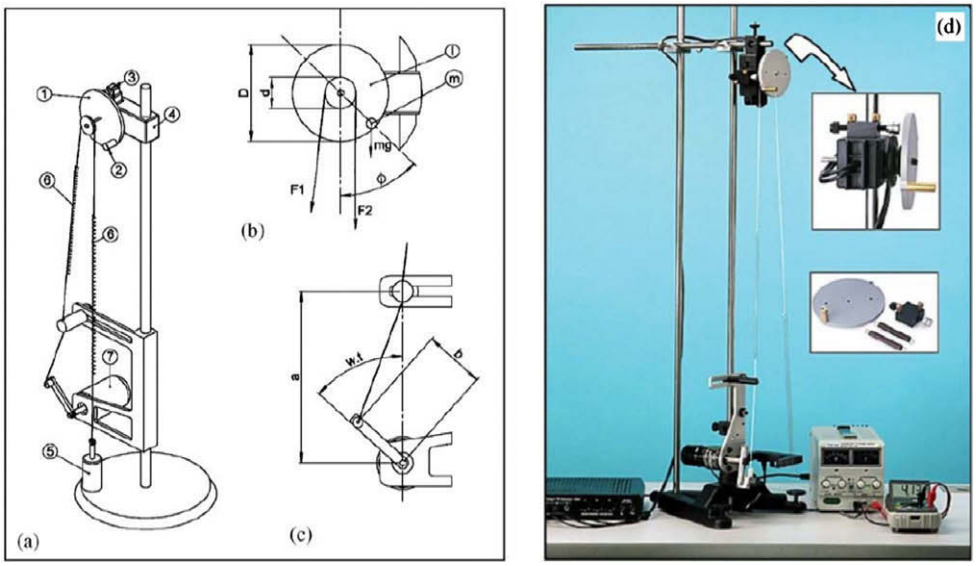

Fig. 1. (a) Nonlinear pendulum – (1) metallic disc; (2) lumped mass; (3) magnetic damping device; (4) rotary motion sensor (PASCO CI-6538); (5) actuator; (6) string-spring device; (7) electric motor (PASCO ME-8750). (b) Parameters and forces on metallic disc. (c) Parameters from driving device. (d) Experimental apparatus.

In order to obtain the equations of motion of the experimental nonlinear pendulum it is assumed that system dissipation may be expressed by a combination of a linear viscous dissipation together with dry friction. Therefore, denoting the angular position as ϕ, the following equation is obtained [22]:

$$\ddot{\phi} + \frac{\zeta}{I}\dot{\phi} + \frac{\mu \mathrm{sgn}(\dot{\phi})}{I} + \frac{kd^2}{2I}\phi + \frac{mgD\sin(\phi)}{2I} = \frac{kd}{2I}\left(\sqrt{a^2 + b^2 - 2ab\cos(\omega t)} - (a-b) - \Delta l\right) \tag{13}$$

where ω is the forcing frequency related to the motor rotation, a defines the position of the guide of the string with respect to the motor, b is the length of the excitation crank of the motor, D is the diameter of the metallic disc and d is the diameter of the driving pulley, m is the lumped mass, ζ represents the linear viscous damping coefficient, while μ is the dry friction coefficient; g is the gravity acceleration, I is the inertia of the disk-lumped mass, k is the string stiffness and Δl is the length variation in the spring provided by the linear actuator (5).

De Paula et al. [22] show that this mathematical model presents results that are in close agreement with experimental data. The pendulum equation can be expressed in terms of Eq. (1) by assuming that $h = kd/2I$, $u = -\Delta l$, f can be obtained from Eqs. (1) and (13), and the term p represents modeling inaccuracies.

4. Controlling the nonlinear pendulum

The controller capability is now investigated by considering numerical simulations. The fourth order Runge–Kutta method is employed and sampling rates of 107 Hz for control system and 214 Hz for dynamical model are assumed. The model parameters are chosen according to De Paula et al. [22]: $I = 1.738 \times 10^{-4}$ kg m^2; $m = 1.47 \times 10^{-2}$ kg; $k = 2.47$ N/m; $\zeta = 2.368 \times 10^{-5}$ kg m^2/s; $\mu = 1.272 \times 10^{-4}$ Nm; $a = 1.6e \times 10^{-1}$ m; $b = 6.0 \times 10^{-2}$ m; $d = 4.8 \times 10^{-2}$ m; $D = 9.5 \times 10^{-2}$ m and $\omega = 5.61$ rad/s.

For tracking purposes, different UPOs are identified using the close return method [17] and two of these are chosen as desired trajectories in the numerical studies that follows.

In order to demonstrate that the adopted control scheme can deal with unstructured uncertainties, the dry friction is treated as unmodeled dynamics and not taken into account within the design of the control law. On this basis, the estimate $\hat{\mu}$ in $\hat{f}$

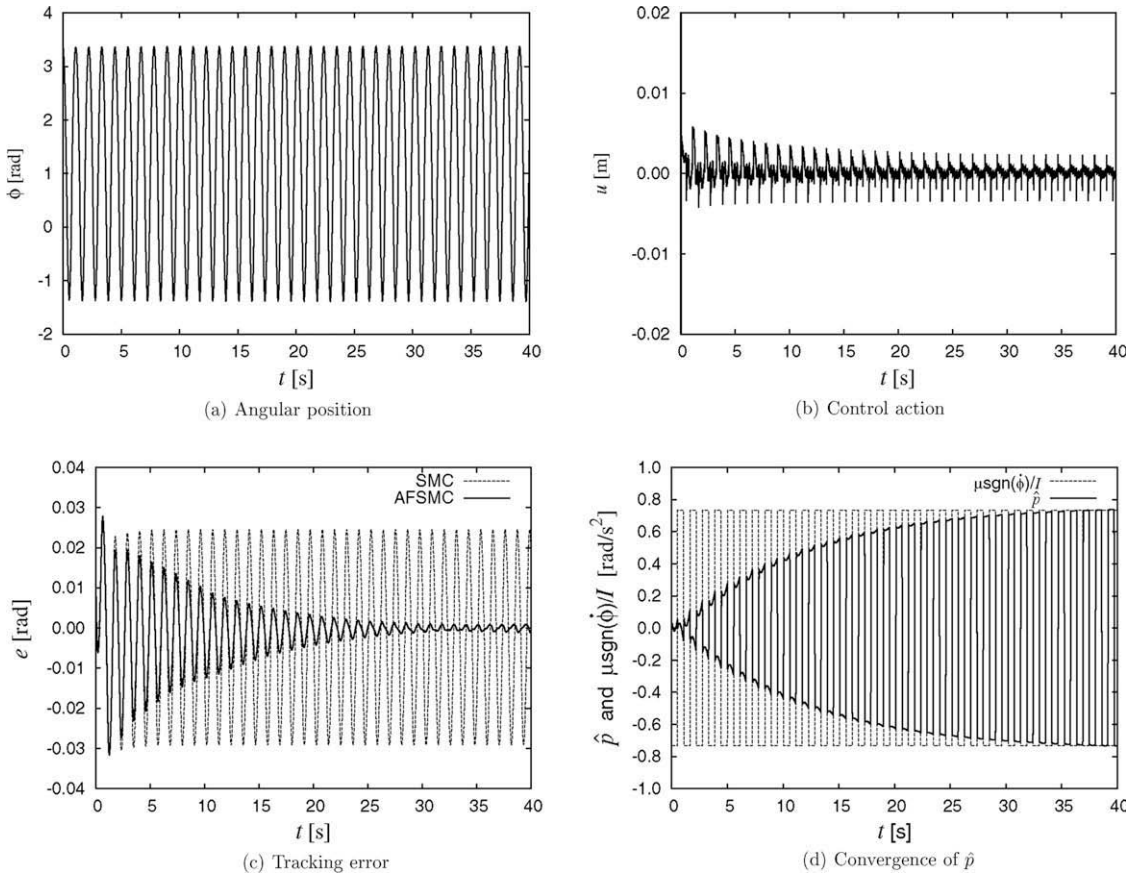

(a) Angular position (b) Control action

(c) Tracking error (d) Convergence of $\hat{p}$

Fig. 2. Tracking of period-1 UPO.

is assumed to vanish, $\hat{\mu} = 0$, but the other estimates in both $\hat{f}$ and $\hat{h}$ are chosen based on the assumption that model coefficients are perfectly known. The other used parameters are $\mathscr{F} = 1.2$; $\mathscr{P} = 1.1$; $\mathscr{H} = 1.0$; $\epsilon = 1.0$; $\lambda = 0.8$; $\eta = 0.05$ and $\varphi = 3.0$.

Concerning the fuzzy system, triangular and trapezoidal membership functions are adopted for both Φ_r and $\dot{\Phi}_r$, with the central values defined, respectively, as $C_0 = \{0.0\}$ and $C_1 = \{-10.0; -1.0; -0.1; 0.0; 0.1; 1.0; 10.0\} \times 10^{-1}$. The chosen fuzzy intersection operator is the product t-norm. It is also important to emphasize that the vector of adjustable parameters is initialized with zero values, $\hat{\mathbf{P}} = \mathbf{0}$, and updated at each iteration step according to the adaptation law, Eq. (8).

Initially, a period-1 UPO is stabilized (Figs. 2 and 3). Fig. 2 shows that the adaptive fuzzy sliding mode controller (AFSMC) is capable to provide the trajectory tracking even in the presence of unstructured uncertainties. It should be emphasized that the control action u, Fig. 2(b), represents the length variation in the string and only tiny variations are required to provide such different dynamic behaviors, which actually allows a great flexibility for the controlled nonlinear system. It can be also verified that the proposed control law provides a smaller tracking error when compared with the conventional sliding mode controller (SMC), Fig. 2(c). For simulation purposes, the AFSMC can be easily converted to the classical SMC by setting the adaptation rate to zero, $\varphi = 0$. The improved performance of AFSMC over SMC is due to its ability to recognize and compensate for modeling imprecisions. Fig. 2(d) presents the convergence of the adaptive fuzzy inference system and the time evolution of its input–output surface is shown in Fig. 3 in four different iteration steps.

At this point, it is assumed that the viscous damping coefficient is not exactly known. The idea is to ratify the robustness of the adopted control scheme against both unstructured uncertainties (or unmodeled dynamics) and structured (or parametric) uncertainties. On this basis, considering a maximal uncertainty of $\pm 20\%$ over the model adopted value, the estimate $\hat{\zeta} = 1.9 \times 10^{-5}$ kg m^2/s is chosen for the computation of $\hat{f}$ in the control law. The other controller parameters are chosen as before. Two different UPOs are now chosen to be stabilized: a period-1 UPO and a period-4 UPO. The obtained results are presented in Figs. 4 and 5.

The idea of the UPO control is interesting since these orbits are embedded in the chaotic attractor and, therefore are natural orbits related to the system dynamics. Hence, it is an important task to evaluate a comparison of the control action required to stabilize some UPOs and a general orbit (artificial or non-natural). Basically, three different situations are treated. In the first case, Fig. 6(a) and (d), a general artificial orbit $[\phi_d, \dot{\phi}_d] = [1.0 + 2.35\sin(2\pi t), 4.70\pi\cos(2\pi t)]$ is considered. A second case, on the other hand, stabilizes a period-1 UPO, Fig. 6(b) and (e). Although both orbits are similar, it should be highlighted that the controller requires less effort to stabilize the UPO. Even with more complicated orbits, as is the case of the period-4 UPO shown in Fig. 6(c), the amplitude of the control action, Fig. 6(f), is significantly smaller when compared with the control effort required to stabilize the general orbit. The control of unstable periodic orbits is the essential aspect to be explored in chaos control that can confer flexibility to the system with low energy consumption.

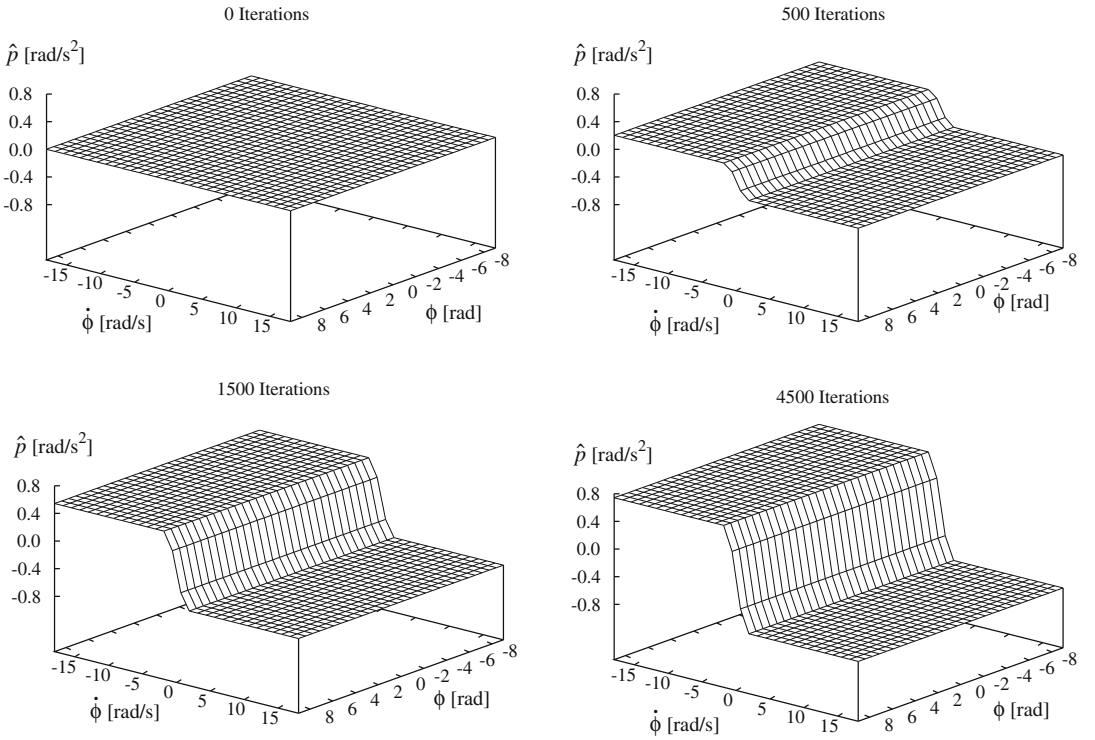

Fig. 3. Convergence of the input–output surface of the fuzzy inference system.

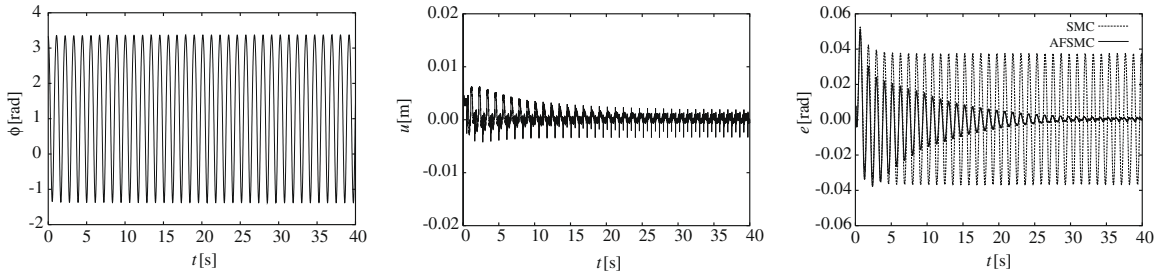

(a) Angular postion (b) Control action (c) Tracking error

Fig. 4. Tracking of period-1 UPO.

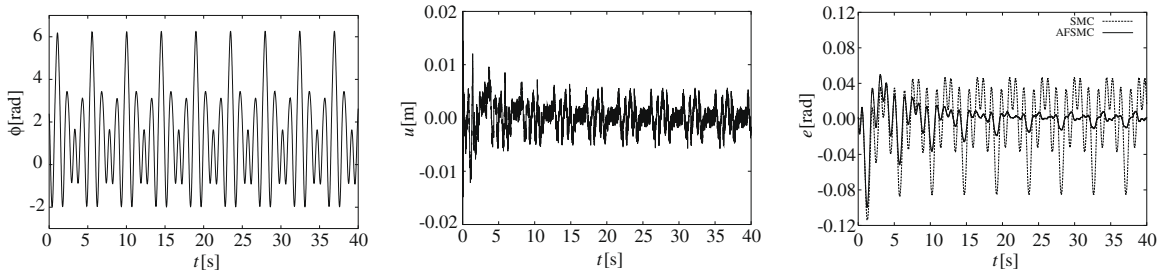

(a) Angular postion (b) Control action (c) Tracking error

Fig. 5. Tracking of period-4 UPO.

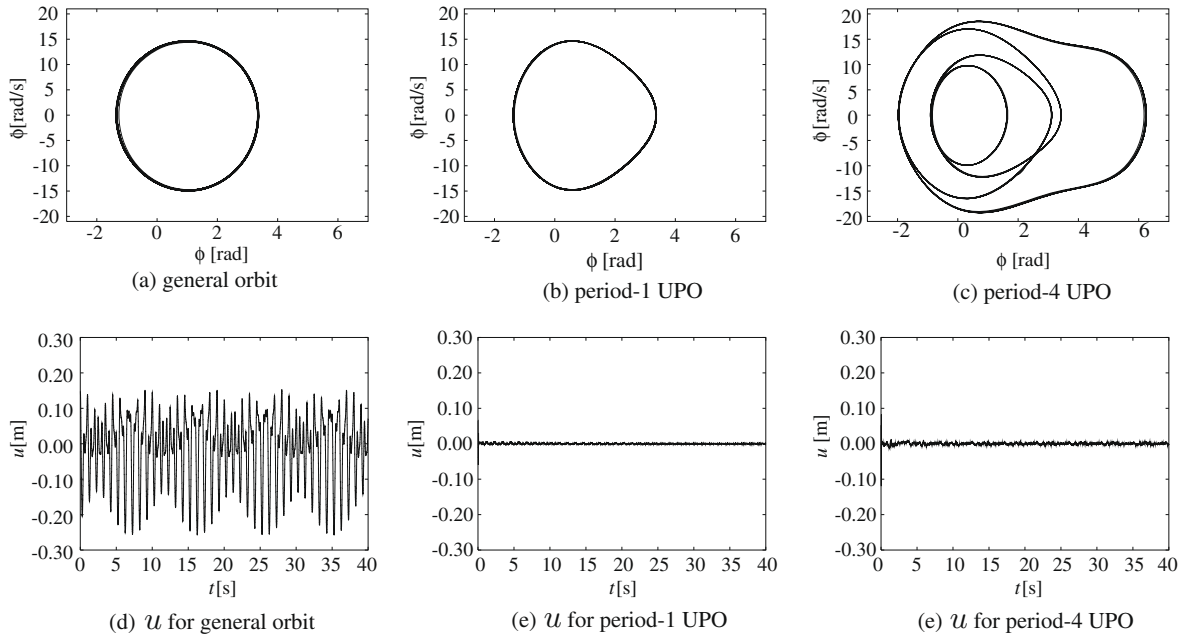

(a) general orbit (b) period-1 UPO (c) period-4 UPO

(d) $\mathcal{U}$ for general orbit (e) $\mathcal{U}$ for period-1 UPO (e) $\mathcal{U}$ for period-4 UPO

Fig. 6. Control action required to stabilize a general orbit and 2 different UPOs.

5. Conclusions

The present contribution presents an adaptive fuzzy sliding mode controller for chaos control. The convergence properties of the tracking error are analytically proven using Lyapunov stability theory and Barbalat's lemma. As an application of the control formulation, numerical simulations of a nonlinear pendulum with chaotic response is of concern. The control

system performance is investigated showing the tracking of a general orbit as well as for UPO stabilization. It is shown that the controller needs less effort to stabilize an UPO when compared with a general non-natural orbit. This is an essential point related to chaos control that can confer flexibility to the system dynamics changing response with low power consumption. The robustness of the proposed control scheme against modeling inaccuracies are investigated evaluating both unstructured and parametric uncertainties. The proposed adaptive controller has an improved performance when compared with the conventional sliding mode controller that are demonstrated in different situations. In general, the proposed procedure is able to perform chaos control even in situations where high uncertainties are involved.

Acknowledgements

The authors acknowledge the support of the Brazilian Research Council (CNPq) and the State of Rio de Janeiro Research Foundation (FAPERJ).

References

[1] Ott E, Grebogi C, Yorke JA. Controlling chaos. Phys Rev Lett 1990;64(11):1196–9.
[2] Pyragas K. Continuous control of chaos by self-controlling feedback. Phys Lett A 1992;170:421–8.
[3] Pyragas K. Delayed feedback control of chaos. Philos Trans R Soc A 2006;364:2309–34.
[4] Dressler U, Nitsche G. Controlling chaos using time delay coordinates. Phys Rev Lett 1992;68(1):1–4.
[5] Hübinger B, Doerner R, Martienssen W, Herdering M, Pitka R, Dressler U. Controlling chaos experimentally in systems exhibiting large effective Lyapunov exponents. Phys Rev E 1994;50(2):932–48.
[6] de Korte RJ, Schouten JC, van den Bleek CMV. Experimental control of a chaotic pendulum with unknown dynamics using delay coordinates. Phys Rev E 1995;52(4):3358–65.
[7] Otani M, Jones AJ. Guiding chaotic orbits, Tech. rep., Imperial College of Science Technology and Medicine, London, 1997.
[8] So P, Ott E. Controlling chaos using time delay coordinates via stabilization of periodic orbits. Phys Rev E 1995;51(4):2955–62.
[9] De Paula AS, Savi MA. A multiparameter chaos control method based on OGY approach. Chaos, Solitons and Fractals. doi:10.1016/j.chaos.2007.09.056.
[10] Savi MA, Pereira-Pinto FHI, Ferreira AM. Chaos control in mechanical systems. Shock Vibr 2006;13(4/5):301–14.
[11] Andrievskii BR, Fradkov AL. Control of chaos: Methods and applications, II – applications. Autom Remote Control 2004;65(4):505–33.
[12] Moon FC, Reddy AJ, Holmes WT. Experiments in control and anti-control of chaos in a dry friction oscillator. J Vibr Control 2003;9(3/4):387–97.
[13] Begley CJ, Virgin LN. On the OGY control of an impact-friction oscillator. J Vibr Control 2001;7(6):923–31.
[14] Hu HY. Controlling chaos of a periodically forced nonsmooth mechanical system. Acta Mechanica Sinica 1995;11(3):251–8.
[15] Spano ML, Ditto WL, Rauseo SN. Exploitation of chaos for active control: an experiment. J Intell Mater Syst Struct 1990;2(4):482–93.
[16] Macau EEN. Exploiting unstable periodic orbits of a chaotic invariant set for spacecraft control. Celestial Mech Dyn Astronomy 2003;87(3):291–305.
[17] Pereira-Pinto FHI, Ferreira AM, Savi MA. Chaos control in a nonlinear pendulum using a semi-continuous method. Chaos, Solitons and Fractals 2004;22(3):653–68.
[18] Pereira-Pinto FHI, Ferreira AM, Savi MA. State space reconstruction using extended state observers to control chaos in a nonlinear pendulum. Int J Bifurcat Chaos 2005;15(12):4051–63.
[19] Wang R, Jing Z. Chaos control of chaotic pendulum system. Chaos, Solitons and Fractals 2004;21(1):201–7.
[20] Yagasaki K, Yamashita S. Controlling chaos using nonlinear approximations for a pendulum with feedforward and feedback control. Int J Bifurcat Chaos 1999;9(1):233–41.
[21] De Paula AS, Savi MA. Chaos control in a nonlinear pendulum using an extended time-delayed feedback method. submitted to Chaos, Solitons and Fractals, 2008.
[22] De Paula AS, Savi MA, Pereira-Pinto FHI. Chaos and transient chaos in an experimental nonlinear pendulum. J Sound Vibr 2006;294:585–95.
[23] Bessa WM, Barrêto RSS. Adaptive fuzzy sliding mode control of uncertain nonlinear systems. Revista Controle & Automačão, accepted for publication.
[24] Bessa WM, Dutra MS, Kreuzer E. Depth control of remotely operated underwater vehicles using an adaptive fuzzy sliding mode controller. Robot Autonom Syst 2008;56:670–7.
[25] Guan P, Liu X-J, Liu J-Z. Adaptive fuzzy sliding mode control for flexible satellite. Eng Appl Artif Intel 2005;18:451–9.
[26] Slotine J-JE. Sliding controller design for nonlinear systems. Int J Control 1984;40(2):421–34.
[27] Bessa WM. Some remarks on the boundedness and convergence properties of smooth sliding mode controllers. Int J Autom Comput 2009;6(2):154–8.
[28] Franca LFP, Savi MA. Distinguishing periodic and chaotic time series obtained from an experimental pendulum. Nonlinear Dyn 2001;26:253–71.